

Effective Interactions and Volume Energies in Charged Colloids: Linear Response Theory

A. R. Denton*

Department of Physics, Acadia University, Wolfville, NS, Canada B0P 1X0

(February 1, 2008)

Interparticle interactions in charge-stabilized colloidal suspensions, of arbitrary salt concentration, are described at the level of effective interactions in an equivalent one-component system. Integrating out from the partition function the degrees of freedom of all microions, and assuming linear response to the macroion charges, general expressions are obtained for both an effective electrostatic pair interaction and an associated microion volume energy. For macroions with hard-sphere cores, the effective interaction is of the DLVO screened-Coulomb form, but with a modified screening constant that incorporates excluded volume effects. The volume energy – a natural consequence of the one-component reduction – contributes to the total free energy and can significantly influence thermodynamic properties in the limit of low-salt concentration. As illustrations, the osmotic pressure and bulk modulus are computed and compared with recent experimental measurements for deionized suspensions. For macroions of sufficient charge and concentration, it is shown that the counterions can act to soften or destabilize colloidal crystals.

PACS numbers: 82.70.Dd, 83.70.Hq, 05.20.Jj, 05.70.-a

I. INTRODUCTION

More than a century ago, it was recognized that most colloidal particles carry an electric charge [1]. Colloidal macroions – typically 1 – 1000 nm in diameter – may acquire charges from surface dissociation of counterions, adsorption of salt ions from solution, or creation of defects in crystal lattices. Electrostatic repulsion between macroions suspended in a molecular fluid is one of the two chief mechanisms by which colloidal suspensions may be stabilized against coagulation induced by attractive van der Waals forces.

Charge-stabilized colloidal suspensions exist in a wide variety of forms. Familiar examples include clay minerals (relevant to mineralogy, agriculture, and the paper industry), paints, inks, and solutions of charged micelles. Further examples are synthetic latex or silica microspheres [2], which may self-assemble, if sufficiently monodisperse, into ordered crystals. Aside from providing valuable model systems for fundamental studies of condensed matter, colloidal crystals exhibit unique optical properties that have inspired a number of recent applications, *e.g.*, nanosecond optical switches [3], chemical sensors [4], and photonic band gap materials [5].

Despite the considerable and growing technological importance of charged colloids, progress in predicting macroscopic properties is limited by an incomplete understanding of interparticle interactions. Most theoretical treatments of electrostatic interactions are rooted in the landmark theory of Derjaguin, Landau, Verwey, and Overbeek (DLVO) [6]. The DLVO theory describes the bare Coulomb interactions between macroions as screened by the surrounding microions (counterions and salt ions). The resulting screened-Coulomb pair potential accounts – at least qualitatively – for a range of observed phenomena, including the dependence of coagulation rate on counterion valence and trends in phase stability with varying salt concentration. Recently, interest in colloidal interactions has intensified as a result of accumulating experimental evidence for apparent long-range attractions between macroions [7,8].

A rigorous statistical mechanical treatment of the multi-component mixture of macroions, counterions, salt ions, and solvent molecules is a daunting task. Interactions in such complex systems are therefore usually treated at the level of *effective* interactions. Tracing out from the partition function statistical degrees of freedom associated with all but a single component, the mixture is formally mapped onto an equivalent one-component system of “pseudo-particles” governed by an effective state-dependent interaction [9]. Effective interactions in charge-stabilized colloids have been modeled by a variety of techniques, including Poisson-Boltzmann cell models [10–12] density-functional theory [13–18], Monte Carlo and Molecular Dynamics simulation [19–22], and powerful *ab initio* methods [13,23].

Here we adopt an alternative approach, recently proposed by Silbert *et al.* [24,25], which exploits analogies between charged colloids and metals. Performing a classical trace over microion degrees of freedom and treating the electrostatic response of the microions to the macroions within second-order perturbation theory, leads to an effective pair interaction between pseudo-macroions and an associated volume energy. The volume energy, which contributes to the total free energy, must be included when calculating thermodynamic properties of charged colloids modeled by

an effective pair potential [14–17,24,29]. Noting the correspondences, microion \leftrightarrow electron and macroion \leftrightarrow metallic ion, the response approach is the colloidal equivalent of the widely-used pseudo-potential theory of metals [26–28].

In previous work [30], the response approach was extended to finite-sized macroions in deionized suspensions. This paper generalizes the theory to the case of arbitrary salt concentration, consistently taking into account (1) the volume excluded to the microions by the macroion hard cores and (2) the response of both counterions and salt ions to the macroion charges. The next section begins with a brief review of the response theory and then outlines our extensions of the theory. Section III presents the main results – obtained within a linear response approximation – for an effective pair potential acting between pseudo-macroions and an associated volume energy, both of which consistently incorporate excluded volume effects. The influence of the volume energy on thermodynamic properties is illustrated by calculations of the osmotic pressure and bulk modulus. Comparisons with experimental data show that the counterions contribute a substantial fraction of the osmotic pressure and can soften or destabilize colloidal crystals. Finally, in Sec. IV we summarize and conclude.

II. THEORY

A. The Model

Within the “primitive” model, the system comprises N_m charged hard-sphere macroions of diameter σ and charge $-Ze$ (e being the elementary charge) and N_c point counterions of charge ze suspended in an electrolyte solvent. Global charge neutrality constrains macroion and counterion numbers according to $ZN_m = zN_c$. Each macroion is assumed to carry a fixed charge, uniformly distributed over its surface. The solvent hosts N_s pairs of salt ions in a uniform dielectric fluid characterized entirely by a dielectric constant ϵ . For notational simplicity, we assume a symmetric 1:1 electrolyte, consisting of N_s point ions of charge ze and N_s of charge $-ze$ (*i.e.*, same valence as counterions). The microions thus number $N_+ = N_c + N_s$ positive and $N_- = N_s$ negative, for a total of $N_\mu = N_c + 2N_s$. The system occupies a total volume V at temperature T and fixed salt concentration maintained by exchange of salt ions, through a semi-permeable membrane, with a salt reservoir.

Denoting macroion and microion coordinates by $\{\mathbf{R}\}$ and $\{\mathbf{r}\}$, respectively, the Hamiltonian of the system may be expressed in the general form

$$H(\{\mathbf{R}\}, \{\mathbf{r}\}) = H_m + H_\mu + H_{m+} + H_{m-}. \quad (1)$$

The first two terms on the right side of Eq. (1) denote Hamiltonians for macroions and microions, respectively. Assuming the only relevant interactions to be steric and electrostatic, the bare macroion Hamiltonian, H_m , is given by

$$H_m = K_m + \frac{1}{2} \sum_{\substack{i,j=1 \\ (i \neq j)}}^{N_m} [v_{\text{HS}}(|\mathbf{R}_i - \mathbf{R}_j|) + v_{\text{mm}}(|\mathbf{R}_i - \mathbf{R}_j|)], \quad (2)$$

K_m being the kinetic energy of the macroions, $v_{\text{HS}}(|\mathbf{R}_i - \mathbf{R}_j|)$ the hard-sphere pair interaction between macroion cores, and $v_{\text{mm}}(r) = Z^2 e^2 / \epsilon r$ the bare Coulomb interaction between a pair of macroions separated by center-to-center distance $r > \sigma$. Similarly, the microion Hamiltonian takes the form

$$\begin{aligned} H_\mu = & K_\mu + \sum_{i=1}^{N_\mu} \sum_{j=1}^{N_m} v_{\text{HS}}(|\mathbf{r}_i - \mathbf{R}_j|) + \frac{1}{2} \sum_{\substack{i,j=1 \\ (i \neq j)}}^{N_+} v_{++}(|\mathbf{r}_i - \mathbf{r}_j|) \\ & + \sum_{i=1}^{N_+} \sum_{j=1}^{N_-} v_{+-}(|\mathbf{r}_i - \mathbf{r}_j|) + \frac{1}{2} \sum_{\substack{i,j=1 \\ (i \neq j)}}^{N_-} v_{--}(|\mathbf{r}_i - \mathbf{r}_j|), \end{aligned} \quad (3)$$

where K_μ is the microion kinetic energy, $v_{\text{HS}}(|\mathbf{r}_i - \mathbf{R}_j|)$ is the hard-sphere interaction between a point microion and a macroion core, and $v_{++}(r) = v_{--}(r) = -v_{+-}(r) = z^2 e^2 / \epsilon r$ is the microion-microion Coulomb interaction. The last two terms in Eq. (1) are the macroion-microion electrostatic interaction energies, given by

$$H_{m\pm} = \sum_{i=1}^{N_\pm} \sum_{j=1}^{N_m} v_{m\pm}(|\mathbf{r}_i - \mathbf{R}_j|), \quad (4)$$

where $v_{m\pm}(r)$ denotes the macroion-microion electrostatic pair interaction. For later reference, we note that Eq. (4) also may be expressed in the form

$$H_{m\pm} = \int d\mathbf{r} \int d\mathbf{R} \rho_{\pm}(\mathbf{r}) \rho_m(\mathbf{R}) v_{m\pm}(|\mathbf{r} - \mathbf{R}|), \quad (5)$$

where

$$\rho_{\pm}(\mathbf{r}) \equiv \sum_{i=1}^{N_{\pm}} \delta(\mathbf{r} - \mathbf{r}_i), \quad \rho_m(\mathbf{R}) \equiv \sum_{j=1}^{N_m} \delta(\mathbf{R} - \mathbf{R}_j) \quad (6)$$

are the microion and macroion density operators, whose Fourier transforms are

$$\hat{\rho}_{\pm}(\mathbf{k}) = \sum_{i=1}^{N_{\pm}} \exp(i\mathbf{k} \cdot \mathbf{r}_i), \quad \hat{\rho}_m(\mathbf{k}) = \sum_{j=1}^{N_m} \exp(i\mathbf{k} \cdot \mathbf{R}_j). \quad (7)$$

Although $v_{m\pm}(r)$ has the Coulomb form outside the macroion core radius, inside the core it has no unique definition. Thus, following van Roij and Hansen [14], we are free to choose $v_{m\pm}(r)$ to be a constant for $r < \sigma/2$ and take

$$v_{m\pm}(r) = \begin{cases} \frac{\pm Z z e^2}{\epsilon r}, & r > \sigma/2 \\ \frac{\pm Z z e^2}{\epsilon \sigma/2} \alpha, & r < \sigma/2, \end{cases} \quad (8)$$

where the parameter α will be specified (Sec. III.C) to ensure that the microion densities vanish within the core.

B. Reduction to an Equivalent One-Component System

With the Hamiltonian specified, we now turn to a statistical mechanical description of the system, our ultimate goal being the free energy. The canonical partition function is given by

$$\mathcal{Z} = \left\langle \exp(-H/k_B T) \right\rangle_{\mu}, \quad (9)$$

the angular brackets symbolizing classical traces over microion and macroion degrees of freedom. Following standard treatments originating from the theory of simple metals [27,28,31], we now reduce the two-component macroion-microion mixture to an equivalent one-component system by performing a restricted trace over microion coordinates, keeping macroion coordinates fixed. Thus, without approximation in this purely classical system,

$$\mathcal{Z} = \langle \exp(-H_{\text{eff}}/k_B T) \rangle_m, \quad (10)$$

where $H_{\text{eff}} \equiv H_m + F_{\mu}$ is the effective Hamiltonian of a one-component system of pseudo-macroions, and where

$$F_{\mu} \equiv -k_B T \ln \langle \exp[-(H_{\mu} + H_{m+} + H_{m-})/k_B T] \rangle_{\mu} \quad (11)$$

may be physically interpreted as the free energy of a nonuniform gas of microions in the midst of macroions fixed at positions \mathbf{R}_i . Formally adding to and subtracting from H the energy, E_b , of a uniform background having a charge equal to that of the macroions, Eq. (11) may be recast in the form

$$F_{\mu} = -k_B T \ln \langle \exp[-(H'_{\mu} + H'_{m+} + H'_{m-})/k_B T] \rangle_{\mu}, \quad (12)$$

where $H'_{\mu} = H_{\mu} + E_b$ and $H'_{m\pm} = H_{m\pm} - E_b/2$. The advantage of this simple manipulation is that H'_{μ} is the Hamiltonian of a classical, two-component plasma of microions, in a uniform compensating background, in the presence of *neutral* hard-sphere macroions. In order that the plasma be free of infinities associated with the long-range Coulomb interaction, the background must occupy the same volume as the microions. The background is thus excluded – along with the microions – from the macroion cores. The microions and background then jointly occupy a *free* volume $V' \equiv V(1 - \eta)$, which is the total volume reduced by the volume fraction of the macroion cores, $\eta = (\pi/6)(N_m/V)\sigma^3$.

The background energy is given explicitly by [31]

$$\begin{aligned}
E_b &= \frac{1}{2}(n_+ - n_-)^2 \int_{V'} d\mathbf{r} \int_{V'} d\mathbf{r}' \frac{z^2 e^2}{\epsilon |\mathbf{r} - \mathbf{r}'|} - \sum_{i=1}^{N_m} \int_{V'} d\mathbf{r} \frac{(n_+ - n_-) Z z e^2}{\epsilon |\mathbf{r} - \mathbf{R}_i|} \\
&= -\frac{1}{2}(N_+ - N_-)(n_+ - n_-) \hat{v}_{++}(0),
\end{aligned} \tag{13}$$

where $n_{\pm} = N_{\pm}/V' = n_{\pm}^{(0)}/(1 - \eta)$ are the *effective* mean densities of microions in the volume not occupied by the macroion cores and $n_{\pm}^{(0)} = N_{\pm}/V$ are the *nominal* mean densities. For later reference, we also define $n_s = n_-$ and $n_c = n_+ - n_-$ as the effective densities of salt-ion pairs and counterions, respectively. In Eq. (13), $\hat{v}_{++}(0)$, defined by

$$\hat{v}_{++}(0) = \int_{V'} d\mathbf{r} \frac{z^2 e^2}{\epsilon r} = \lim_{k \rightarrow 0} \left(\frac{4\pi z^2 e^2}{\epsilon k^2} \right), \tag{14}$$

is the $k \rightarrow 0$ limit of the Fourier transform of $v_{++}(r)$. Although formally infinite, E_b will be seen below to be identically cancelled by compensating infinities in H_{μ} and $H_{m\pm}$.

C. Linear Response Approximation

The theory presented thus far is exact, within the primitive model. The challenge remains to calculate the microion free energy [Eq. (11)]. One proposed strategy [14] invokes density-functional theory to approximate F_{μ} , regarded as a functional of the microion densities, by performing a functional Taylor-series expansion about a uniform microion plasma. An alternative strategy [24,25], inspired by the pseudo-potential theory of metals, is to formally regard $H'_{m\pm}$ as “external” potentials acting upon a microion plasma and then approximate F_{μ} by perturbation theory. Following the second strategy, we write [31]

$$F_{\mu} = F_p + \int_0^1 d\lambda (\langle H'_{m+} \rangle_{\lambda} + \langle H'_{m-} \rangle_{\lambda}), \tag{15}$$

where

$$F_p = -k_B T \ln \langle \exp(-H'_{\mu}/k_B T) \rangle_{\mu} \tag{16}$$

is the free energy of the reference microion plasma, occupying a volume V' , in the presence of neutral hard-sphere macroions. The integral over λ in Eq. (15) corresponds physically to an adiabatic charging of the macroions from neutral to fully-charged spheres. The ensemble average $\langle \rangle_{\lambda}$ represents an average with respect to the distribution function of a system whose macroions carry a charge λZ .

Further progress is facilitated by expressing $\langle H'_{m\pm} \rangle_{\lambda}$ in terms of Fourier components of the macroion and microion densities and of the macroion-microion interaction. From Eqs. (5)-(7), we have

$$\langle H'_{m\pm} \rangle_{\lambda} = \frac{1}{V'} \sum_{\mathbf{k} \neq 0} \hat{v}_{m\pm}(\mathbf{k}) \langle \hat{\rho}_{\pm}(\mathbf{k}) \rangle_{\lambda} \hat{\rho}_m(-\mathbf{k}) + \frac{1}{V'} \lim_{k \rightarrow 0} [\hat{v}_{m\pm}(k) \langle \hat{\rho}_{\pm}(\mathbf{k}) \rangle_{\lambda} \hat{\rho}_m(-\mathbf{k})] - E_b/2. \tag{17}$$

Evidently $\langle H'_{m\pm} \rangle_{\lambda}$ depends through $\hat{\rho}_{\pm}(\mathbf{k})$ upon the response of the microions to the macroion charge density. Regarding the macroion charge as imposing an external potential on the microions, and assuming that the microion densities respond *linearly* to this potential, the Fourier components of the microion densities appearing in Eq. (17) may be expressed in the form

$$\langle \hat{\rho}_+(\mathbf{k}) \rangle_{\lambda} = \lambda [\chi_{++}(k) - \chi_{+-}(k)] \hat{v}_{m+}(k) \hat{\rho}_m(\mathbf{k}), \quad k \neq 0, \tag{18}$$

and

$$\langle \hat{\rho}_-(\mathbf{k}) \rangle_{\lambda} = \lambda [\chi_{+-}(k) - \chi_{--}(k)] \hat{v}_{m+}(k) \hat{\rho}_m(\mathbf{k}), \quad k \neq 0, \tag{19}$$

where $\chi_{\pm\pm}(k)$ are the linear response functions of the reference two-component microion plasma and where we have used the symmetry relations $\chi_{+-}(k) = \chi_{-+}(k)$ and $\hat{v}_{m+}(k) = -\hat{v}_{m-}(k)$. Note that for $k = 0$ there is no response, since $\hat{\rho}_{\pm}(0) = N_{\pm}$, as determined by the fixed numbers of microions. Substituting Eqs. (18) and (19) into Eq. (17) and this in turn into Eq. (15), and integrating over λ , the microion free energy is given to second order in the macroion-microion interaction by

$$\begin{aligned}
F_\mu &= F_p + \frac{1}{2V'} \sum_{\mathbf{k} \neq 0} [\chi_{++}(k) - 2\chi_{+-}(k) + \chi_{--}(k)] [\hat{v}_{m+}(k)]^2 \hat{\rho}_m(\mathbf{k}) \hat{\rho}_m(-\mathbf{k}) \\
&+ N_m(n_+ - n_-) \lim_{k \rightarrow 0} [\hat{v}_{m+}(k)] - E_b,
\end{aligned} \tag{20}$$

where again we have used the relation $\hat{v}_{m+}(k) = -\hat{v}_{m-}(k)$. Correspondingly, the effective Hamiltonian takes the form

$$\begin{aligned}
H_{\text{eff}} &= K_m + \frac{1}{2} \sum_{\substack{i,j=1 \\ i \neq j}}^{N_m} v_{\text{HS}}(|\mathbf{R}_i - \mathbf{R}_j|) + \frac{1}{2V'} \sum_{\mathbf{k}} \hat{v}_{mm}(k) [\hat{\rho}_m(\mathbf{k}) \hat{\rho}_m(-\mathbf{k}) - N_m] \\
&+ F_p + \frac{1}{2V'} \sum_{\mathbf{k} \neq 0} \chi(k) [\hat{v}_{m+}(k)]^2 \hat{\rho}_m(\mathbf{k}) \hat{\rho}_m(-\mathbf{k}) + N_m(n_+ - n_-) \lim_{k \rightarrow 0} [\hat{v}_{m+}(k)] - E_b,
\end{aligned} \tag{21}$$

where we have defined

$$\chi(k) \equiv \chi_{++}(k) - 2\chi_{+-}(k) + \chi_{--}(k). \tag{22}$$

Now rearranging terms, Eq. (21) may be restructured and written in the formally simpler form

$$\begin{aligned}
H_{\text{eff}} &= K_m + \frac{1}{2} \sum_{\substack{i,j=1 \\ i \neq j}}^{N_m} v_{\text{HS}}(|\mathbf{R}_i - \mathbf{R}_j|) + \frac{1}{2V'} \sum_{\mathbf{k}} \hat{v}_{\text{eff}}(k) [\hat{\rho}_m(\mathbf{k}) \hat{\rho}_m(-\mathbf{k}) - N_m] + E_0 \\
&= K_m + \frac{1}{2} \sum_{\substack{i,j=1 \\ i \neq j}}^{N_m} [v_{\text{HS}}(|\mathbf{R}_i - \mathbf{R}_j|) + v_{\text{eff}}(|\mathbf{R}_i - \mathbf{R}_j|)] + E_0,
\end{aligned} \tag{23}$$

where

$$v_{\text{eff}}(r) = v_{\text{mm}}(r) + v_{\text{ind}}(r) \tag{24}$$

has the physical interpretation of an *effective* electrostatic pair potential between pseudo-macroions, which is the sum of the bare Coulomb potential and an *induced* potential whose Fourier transform is

$$\hat{v}_{\text{ind}}(k) = \chi(k) [\hat{v}_{m+}(k)]^2. \tag{25}$$

The final term in Eq. (23) is the *volume energy*,

$$E_0 = F_p + \frac{N_m}{2} \lim_{r \rightarrow 0} v_{\text{ind}}(r) + N_m(n_+ - n_-) \lim_{k \rightarrow 0} \left[-\frac{z}{2Z} \hat{v}_{\text{ind}}(k) + \hat{v}_{m+}(k) \right] - E_b, \tag{26}$$

which is a natural byproduct of the reduction to an equivalent one-component system. Although it has no explicit dependence on the macroion coordinates (see below), E_0 evidently depends on the mean density of macroions and therefore can contribute significantly to the total free energy of the system. In passing, we note that the above expressions for the effective pair potential and the volume energy are analogous to expressions appearing in the pseudo-potential theory of metals [27,28,31,32] if one substitutes for F_p and $\chi(k)$, respectively, the energy and linear response function of the homogeneous electron gas (in the presence of a compensating background), and for $\hat{v}_{m+}(k)$ the electron-ion pseudo-potential.

Summarizing thus far, we have adopted the primitive model of charged colloids, formally reduced the macroion-microion mixture to an equivalent one-component system of pseudo-macroions, and applied a linear response approximation to the microion density, to obtain expressions for an effective electrostatic pair interaction [Eqs. (24) and (25)] and an associated volume energy [Eq. (26)]. Practical calculations still require explicit specification of (1) the reference plasma free energy F_p , (2) the plasma linear response functions $\chi_{\pm\pm}(k)$, and (3) the macroion-microion interaction $\hat{v}_{m+}(k)$. In the next section we consider each of these in turn.

III. RESULTS AND DISCUSSION

A. Reference Microion Plasma

The free energy of the two-component reference plasma may be expressed as

$$F_p = F_{id} + F_{corr} + F_{cc} - E_b, \quad (27)$$

where F_{id} and F_{corr} are the ideal-gas and correlation contributions and F_{cc} is the energy associated with Coulomb pair interactions between microions. It is important to emphasize that by associating the hard-sphere part of the total macroion-microion interaction with the microion Hamiltonian [Eq. (3)] – required, since response theory does not apply to hard-sphere interactions – the reference microion plasma is implicitly restricted to the free volume outside of the macroion cores. As a consequence, the plasma is not strictly uniform, since the boundary conditions, imposed by the macroion surfaces, may induce nonuniformity. In general, the ideal-gas free energy is given by

$$\beta F_{id} = \int d\mathbf{r} \rho_+^{(0)}(\mathbf{r}) \left(\ln[\rho_+^{(0)}(\mathbf{r})\Lambda^3] - 1 \right) + \int d\mathbf{r} \rho_-^{(0)}(\mathbf{r}) \left(\ln[\rho_-^{(0)}(\mathbf{r})\Lambda^3] - 1 \right), \quad (28)$$

where $\beta \equiv 1/k_B T$, Λ is the microion thermal de Broglie wavelength, and $\rho_{\pm}^{(0)}(\mathbf{r})$ are the nonuniform densities of positive and negative microions in an external field due to the macroion cores (but *not* their electric fields).

Now, for typical macroion charges and concentrations, counterion concentrations are in the μM (10^{-6} mol/l) range. If the salt concentration also falls in this range, then microion concentrations are low enough that the plasma is essentially uniform. In this case, $F_{cc} \simeq E_b$ and the last two terms in Eq. (27) cancel each other. Furthermore, a plasma of such low concentration is weakly coupled, with coupling parameter $\Gamma \equiv z^2 e^2 / \epsilon k_B T a_\mu \ll 1$, where $a_\mu = (3/4\pi n_\mu)^{1/3}$ is the microion sphere radius and $n_\mu = n_+ + n_-$ is the total microion number density. (In sharp contrast, electron plasmas in metals are typically characterized by $\Gamma \gg 1$.) The correlation free energy per microion then may be approximated by the Abe expansion [33]

$$\frac{\beta F_{corr}}{N_\mu} = -\frac{1}{\sqrt{3}} \Gamma^{3/2} + O(\Gamma^3), \quad (29)$$

the leading term being the Debye-Hückel approximation [34]. Thus, at low salt concentrations, if nonuniformities and correlations are ignored [14,17,29], a reasonable approximation for the free energy of the microion plasma is

$$\begin{aligned} \beta F_p &\simeq N_+ [\ln(n_+ \Lambda^3) - 1] + N_- [\ln(n_- \Lambda^3) - 1] \\ &= N_\mu [\ln(n_\mu \Lambda^3) - 1 + x_+ \ln x_+ + x_- \ln x_-], \end{aligned} \quad (30)$$

where $x_{\pm} = N_{\pm}/N_\mu$ are the mean microion concentrations.

B. Linear Response Functions

The linear response functions, $\chi_{ij}(k)$, $i, j = \pm$, of the two-component reference plasma are simply proportional to the corresponding partial structure factors, $S_{ij}(k)$:

$$\chi_{ij}(k) = -\beta n_\mu S_{ij}(k). \quad (31)$$

Liquid state theory [35] now relates the partial structure factors to Fourier transforms of the pair correlation functions, $\hat{h}_{ij}(k)$, via

$$S_{ij}(k) = x_i \delta_{ij} + x_i x_j n_\mu \hat{h}_{ij}(k). \quad (32)$$

The pair correlation functions are in turn related to Fourier transforms of the direct correlation functions, $\hat{c}_{ij}(k)$, by the Ornstein-Zernike (OZ) equation for mixtures:

$$\hat{h}_{ij}(k) = \hat{c}_{ij}(k) + n_\mu \sum_l x_l \hat{c}_{il}(k) \hat{h}_{lj}(k), \quad i, j, l = \pm \quad (33)$$

which serves in fact to define $\hat{c}_{ij}(k)$. For such weakly-coupled plasmas as we encounter in charged colloids, the mean spherical approximation (MSA) provides a reasonable closure for the OZ equation. This amounts to approximating $c_{ij}(r)$ by its asymptotic ($r \rightarrow \infty$) limit, $c_{ij}(r) \simeq -\beta v_{ij}(r)$, for all r , or equivalently,

$$\hat{c}_{ij}(k) \simeq -\beta \hat{v}_{ij}(k) = -\frac{4\pi\beta z_i z_j e^2}{\epsilon k^2}, \quad (34)$$

where $z_i, z_j = \pm z$. Since, in the MSA, $\hat{c}_{++}(k) = \hat{c}_{--}(k) = -\hat{c}_{+-}(k) \equiv \hat{c}(k)$, it follows directly from Eq. (33) that

$$\hat{h}_{++}(k) = \hat{h}_{--}(k) = -\hat{h}_{+-}(k) = \frac{\hat{c}(k)}{1 - n_\mu \hat{c}(k)}. \quad (35)$$

Substituting Eqs. (32), (34), and (35) into Eq. (31) yields $\chi_{ij}(k)$, from which we obtain

$$\chi_{++}(k) - \chi_{+-}(k) = -\frac{\beta n_+}{1 - n_\mu \hat{c}(k)} = -\frac{\beta n_+}{1 + \kappa^2/k^2}, \quad (36)$$

$$\chi_{+-}(k) - \chi_{--}(k) = \frac{\beta n_-}{1 - n_\mu \hat{c}(k)} = \frac{\beta n_-}{1 + \kappa^2/k^2}, \quad (37)$$

and

$$\chi(k) = -\frac{\beta n_\mu}{1 - n_\mu \hat{c}(k)} = -\frac{\beta n_\mu}{1 + \kappa^2/k^2}, \quad (38)$$

where

$$\kappa \equiv \left(\frac{4\pi n_\mu z^2 e^2}{\epsilon k_B T} \right)^{1/2} = \left(\frac{4\pi n_\mu^{(0)} z^2 e^2}{(1 - \eta) \epsilon k_B T} \right)^{1/2}, \quad (39)$$

and $n_\mu^{(0)} = N_\mu/V = n_\mu(1 - \eta)$ is the total nominal microion number density. As will be seen below, the parameter κ plays the role of the Debye screening constant (inverse screening length) in the microion density profiles and in the effective pair interaction.

C. Microion Density Profiles

Specifying the macroion-microion interaction amounts to determining the value of the parameter α in Eq. (8) that ensures vanishing microion densities inside the macroion cores. This in turn requires a calculation of the real-space microion density profiles. The first step of this calculation is to Fourier transform Eq. (8), with the result

$$\hat{v}_{m\pm}(k) = \mp \frac{4\pi Z z e^2}{\epsilon k^2} \left[(1 - \alpha) \cos(k\sigma/2) + \alpha \frac{\sin(k\sigma/2)}{k\sigma/2} \right]. \quad (40)$$

Now substituting Eqs. (36), (37), and (40) into Eqs. (18) and Eqs. (19) gives for the $k \neq 0$ Fourier components of the microion densities

$$\hat{\rho}_\pm(\mathbf{k}) = \pm x_\pm \frac{Z}{z} \left(\frac{\kappa^2}{k^2 + \kappa^2} \right) \left[(1 - \alpha) \cos(k\sigma/2) + \alpha \frac{\sin(k\sigma/2)}{k\sigma/2} \right] \sum_{j=1}^{N_m} \exp(i\mathbf{k} \cdot \mathbf{R}_j), \quad k \neq 0, \quad (41)$$

where the sum is over the positions \mathbf{R}_j of the macroions. Next inverse transforming Eq. (41), while respecting the $k \rightarrow 0$ limits, $\hat{\rho}_\pm(0) = N_\pm$, we obtain

$$\rho_\pm(\mathbf{r}) = \begin{cases} \rho_\infty \pm x_\pm \sum_{j=1}^{N_m} \rho_{>}(|\mathbf{r} - \mathbf{R}_j|), & |\mathbf{r} - \mathbf{R}_j| > \sigma/2 \\ x_\pm \sum_{j=1}^{N_m} \rho_{<}(|\mathbf{r} - \mathbf{R}_j|), & |\mathbf{r} - \mathbf{R}_j| < \sigma/2, \end{cases} \quad (42)$$

where $\rho_\infty = x_- n_+ + x_+ n_-$ is the bulk density of positive or negative microions (far from any macroion). Note that in general $\rho_\infty \neq n_s$, although $\rho_\infty \rightarrow n_s$ in the limit $x_\pm \rightarrow 1/2$ ($n_c/n_s \rightarrow 0$). In Eq. (42), $\rho_{>}(r)$ and $\rho_{<}(r)$ are single-macroion orbitals, given by

$$\rho_{>}(r) = \frac{Z}{z} \frac{\kappa^2}{4\pi} \left[(1 - \alpha) \cosh(\kappa\sigma/2) + \alpha \frac{\sinh(\kappa\sigma/2)}{\kappa\sigma/2} \right] \frac{\exp(-\kappa r)}{r}, \quad r > \sigma/2, \quad (43)$$

and

$$\rho_{<}(r) = \frac{Z}{z} \frac{\kappa^2}{4\pi} \left(-1 + \alpha + \frac{\alpha}{\kappa\sigma/2} \right) \exp(-\kappa\sigma/2) \frac{\sinh(\kappa r)}{r}, \quad r < \sigma/2. \quad (44)$$

Vanishing of $\rho_{<}(r)$ for $r < \sigma/2$ is evidently ensured by setting

$$\alpha = \frac{\kappa\sigma/2}{1 + \kappa\sigma/2}. \quad (45)$$

Finally, substituting this choice for α back into Eq. (43) specifies the $r > \sigma/2$ orbital as

$$\rho_{>}(r) = \frac{Z}{z} \frac{\kappa^2}{4\pi} \frac{\exp(\kappa\sigma/2)}{1 + \kappa\sigma/2} \frac{\exp(-\kappa r)}{r}, \quad r > \sigma/2, \quad (46)$$

which is automatically normalized to the correct number of counterions per macroion (Z/z). The corresponding microion density profiles are the linear combinations

$$\rho_{\pm}(\mathbf{r}) = \rho_{\infty} \pm x_{\pm} \frac{Z}{z} \frac{\kappa^2}{4\pi} \frac{\exp(\kappa\sigma/2)}{1 + \kappa\sigma/2} \sum_{j=1}^{N_m} \frac{\exp(-\kappa|\mathbf{r} - \mathbf{R}_j|)}{|\mathbf{r} - \mathbf{R}_j|}, \quad |\mathbf{r} - \mathbf{R}_j| > \sigma/2. \quad (47)$$

Expression (46) is seen to be of precisely the same form as the Debye-Hückel expression for the density of electrolyte ions around a macroion [1]. A significant distinction lies, however, in the definition of the screening constant, κ . Whereas the Debye-Hückel κ depends on the *nominal* bulk density of electrolyte ions, our κ [Eq. (39)] depends rather on the *effective* mean microion density n_{μ} (in the volume unoccupied by macroions). The importance of redefining the usual κ in this way, particularly for concentrated suspensions, has been noted previously by Russel and coworkers [36].

D. Effective Pair Interaction and Volume Energy

We are now in a position to derive the main results of the paper. Considering first the effective electrostatic pair interaction between pseudo-macroions, we proceed by substituting Eq. (45) into Eq. (40), obtaining for the macroion-microion interaction

$$\hat{v}_{m\pm}(k) = \mp \frac{4\pi Z z e^2}{\epsilon k^2} \left(\frac{1}{1 + \kappa\sigma/2} \right) \left[\cos(k\sigma/2) + \kappa \frac{\sin(k\sigma/2)}{k} \right]. \quad (48)$$

Next substituting Eqs. (38) and (48) into Eq. (25) yields the induced potential:

$$\hat{v}_{\text{ind}}(k) = - \frac{2\pi Z^2 e^2}{\epsilon k^2} \left(\frac{1}{1 + \kappa\sigma/2} \right)^2 \left(\frac{\kappa^2}{k^2 + \kappa^2} \right) \left[1 + \cos(k\sigma) + 2\kappa \frac{\sin(k\sigma)}{k} + \kappa^2 \frac{1 - \cos(k\sigma)}{k^2} \right]. \quad (49)$$

Fourier transformation of Eq. (49) is a straightforward calculation, with the result

$$v_{\text{ind}}(r) = \begin{cases} \frac{Z^2 e^2}{\epsilon} \left(\frac{\exp(\kappa\sigma/2)}{1 + \kappa\sigma/2} \right)^2 \frac{\exp(-\kappa r)}{r} - \frac{Z^2 e^2}{\epsilon r}, & r > \sigma \\ - \frac{Z^2 e^2}{2\epsilon r} \left(\frac{1}{1 + \kappa\sigma/2} \right)^2 \left[(2 + \kappa\sigma)\kappa r - \frac{1}{2}\kappa^2 r^2 \right], & r < \sigma. \end{cases} \quad (50)$$

Finally, substituting Eq. (50) into Eq. (24), we obtain an explicit expression for the effective electrostatic pair potential:

$$v_{\text{eff}}(r) = \frac{Z^2 e^2}{\epsilon} \left(\frac{\exp(\kappa\sigma/2)}{1 + \kappa\sigma/2} \right)^2 \frac{\exp(-\kappa r)}{r}, \quad r > \sigma. \quad (51)$$

This result is seen to be identical in form to the electrostatic part of the DLVO effective pair potential [6], which is usually derived by linearizing the Poisson-Boltzmann equation. The only distinction between our pair potential and

the DLVO potential lies in the definition of the screening constant, ours [Eq. (39)] being a factor $(1 - \eta)^{-1/2}$ larger than the usual DLVO κ to account for exclusion of microions from the macroion cores.

Now the volume energy may be explicitly determined from Eq. (26). It follows immediately from Eq. (50) that

$$\lim_{r \rightarrow 0} v_{\text{ind}}(r) = - \frac{Z^2 e^2}{\epsilon} \frac{\kappa}{1 + \kappa \sigma / 2}, \quad (52)$$

from Eq. (49) that

$$\lim_{k \rightarrow 0} \hat{v}_{\text{ind}}(k) = - \left(\frac{Z}{z} \right)^2 \hat{v}_{++}(0) + \frac{\pi Z^2 e^2 \sigma^2}{\epsilon} \frac{1 + \kappa \sigma / 6}{1 + \kappa \sigma / 2} + \frac{4\pi Z^2 e^2}{\epsilon \kappa^2}, \quad (53)$$

and from Eq. (48) that

$$\lim_{k \rightarrow 0} \hat{v}_{m+}(k) = - \frac{Z}{z} \hat{v}_{++}(0) + \frac{\pi Z z e^2 \sigma^2}{2\epsilon} \frac{1 + \kappa \sigma / 6}{1 + \kappa \sigma / 2}. \quad (54)$$

Substituting Eqs. (52) – (54) into Eq. (26), and using approximation (30), we obtain for the volume energy

$$\beta E_0 = N_+ \ln(n_+ \Lambda^3) + N_- \ln(n_- \Lambda^3) - N_m \frac{Z^2 e^2 \beta}{2\epsilon} \frac{\kappa}{1 + \kappa \sigma / 2} - \frac{1}{2} \frac{(N_+ - N_-)^2}{N_+ + N_-}, \quad (55)$$

neglecting irrelevant constants. Note that the infinities associated with the $k \rightarrow 0$ limits formally cancel one another, as they must [37]. The first term on the right side of Eq. (55) is the ideal-gas plasma free energy, discussed in Sec. III A. The second term, which accounts for the electrostatic energy of interaction between the macroions and their screening clouds of counterions, is equivalent to one half the interaction energy were all the counterions to be placed at a radial distance κ^{-1} from the centers of their respective macroions. The final term corresponds to the $k \rightarrow 0$ limit in Eq. (26). Our result for the volume energy is very similar to that derived by van Roij *et al.* [14,15] from a density-functional expansion, differing only in the manner in which exclusion of microions from the macroion cores is incorporated. While Eq. (55) incorporates excluded volume effects through a dependence of the screening constant [Eq. (39)] on the effective microion density, van Roij *et al.* incorporate them through an additional term in the volume energy [Eq. (61) in Ref. [15]].

In closing this section, we remark on the range of validity of the theory. First, although the linear response approximation presupposes relatively weak microion response to the macroions, and thus weak screening, the general form of the screened-Coulomb pair potential in bulk suspensions is broadly supported by Poisson-Boltzmann cell model calculations [10], *ab initio* simulations [13,23], and experiments [7]. Second, the excluded volume corrections incorporated in the modified screening constant, κ , may become significant even in the weak-screening regime for concentrated suspensions of weakly charged macroions. Finally, although the theory neglects (in mean-field fashion) fluctuations and correlations in the microion densities, Monte Carlo simulations and cell model calculations [44] for spherical macroions suggest that such correlations contribute only marginally to the total free energy.

E. Osmotic Pressure and Bulk Modulus

Being independent of the macroion coordinates, the microion volume energy, E_0 , appears simply as an additive term in the total Helmholtz free energy of the system: $F = F_m + E_0$, where F_m is the free energy of the equivalent one-component system of pseudo-macroions interacting via the effective pair potential $v_{\text{eff}}(r)$. Correspondingly, any thermodynamic quantity derived from this free energy may be decomposed into effective macroion and microion contributions. Since E_0 [Eq. (55)] depends on the mean macroion density – both explicitly and implicitly through κ – it can significantly influence thermodynamic properties of the system, especially at low salt concentrations [15–17,30].

As illustrations, we consider the osmotic pressure and bulk modulus. A colloidal suspension in equilibrium, through a semi-permeable membrane, with a reservoir of salt solution exerts an osmotic pressure, $\Pi = P - P_r$, defined as the difference between the pressure of the system, P , and that of the reservoir, P_r . Treating the reservoir as an ideal gas of N_r salt ion pairs in a volume V_r , we have $\beta P_r = 2N_r/V_r$. Chemical equilibrium is characterized by equality of the chemical potentials of salt ion species exchanged between the system and the reservoir. The chemical potential of the salt, defined as the change in free energy upon adding a salt ion, includes a contribution arising from the effect of salt concentration on the macroion-macroion interaction (through κ). Thus, in general, the salt concentrations of the system and reservoir are nontrivially related. However, for systems sufficiently dilute that the macroion contribution

may be ignored – an assumption we make here – the condition for chemical equilibrium may be approximated by equality of the reservoir salt density, N_r/V_r , and the *effective* salt density of the system, $n_s = (N_s/V)/(1 - \eta)$. Note that the effective salt density exceeds the nominal salt density, N_s/V , by the ratio of the total volume to the free volume unoccupied by the macroion cores. The distinction here between nominal and reservoir salt densities is akin to that between nominal and reservoir polymer densities in colloid-polymer mixtures [38]. The reservoir pressure is then given by

$$\beta P_r \simeq 2n_s. \quad (56)$$

The total pressure (or equation of state) of the system, $P = P_m + P_0$, comprises a macroion contribution, P_m , and a microion contribution, $P_0 = -(\partial E_0/\partial V)_{N_m, N_s}$. Combining Eqs. (55) and (56), we obtain

$$\beta \Pi \sigma^3 = \beta P_m \sigma^3 + n_c \sigma^3 - \frac{1}{16\pi} \frac{Z}{z^2} \frac{(\kappa\sigma)^3}{(1 + \kappa\sigma/2)^2}. \quad (57)$$

The same result is obtained for arbitrary macroion concentration in the limit of zero salt concentration ($n_s \rightarrow 0$), in which case $P_r = 0$. The second and third terms in Eq. (57) represent, respectively, the ideal-gas pressure of the counterions and a van der Waals-like adjustment that accounts for the attraction between counterions and macroions. With increasing counterion density, these two terms compete with each other, the attractive term acting to reduce the total osmotic pressure. For weak microion screening ($\kappa\sigma < 1$), where the electrostatic fields of the macroions are relatively weak and the microion densities close to uniform, Eq. (57) should reasonably approximate the osmotic pressure. In fact, in the limit $\kappa\sigma \rightarrow 0$, our result naturally tends to the correct ideal-gas limit, $\beta P_0 \rightarrow n_c$. For stronger screening ($\kappa\sigma > 1$), where the microion densities are more nonuniform, nonlinear response effects may become significant.

The bulk modulus (or inverse compressibility), defined by $B \equiv -V(\partial \Pi/\partial V)_{N_m, N_s}$, may be similarly expressed in the form $B = B_m + B_0$, where B_m and B_0 are the macroion and microion contributions, respectively. From Eq. (57), we immediately obtain

$$\beta B \sigma^3 = \beta B_m \sigma^3 + \frac{n_c \sigma^3}{1 - \eta} - \frac{3}{32\pi} \frac{Z}{z^2} \frac{1}{1 - \eta} \frac{(\kappa\sigma)^3(1 + \kappa\sigma/6)}{(1 + \kappa\sigma/2)^3}, \quad (58)$$

which again includes repulsive and attractive microion terms. In Eqs. (57) and (58), the macroion contributions, P_m and B_m , are understood to be obtained from a theory (or simulation) of a one-component system of particles interacting via the effective pair potential [Eqs. (39) and (51)]. In practice, the macroion charge, notoriously difficult to extract from experiment, is usually replaced by an adjustable parameter, the effective or renormalized charge, Z^* [10].

As a test of our results, we compare, in Fig. 1, the osmotic pressure predicted from Eq. (57) with the recent experimental measurements of Reus *et al.* [39] for a colloidal fcc crystal in a highly deionized ($n_s = 0$) aqueous solvent at room temperature (Bjerrum length $\lambda_B \equiv \beta z^2 e^2/\epsilon = 0.714$ nm). As an approximation for the macroion pressure, P_m , we use results of integral-equation calculations based on the virial equation with HNC closure for the liquid-state pair distribution function [39,40]. For the effective macroion charge, we take the value $Z^* = 700$ estimated by Reus *et al.* to best match their phase diagram to the simulations of Robbins *et al.* [41].

The microion contribution is seen to make the dominant contribution to the total osmotic pressure and to substantially improve the agreement between the one-component model and experiment, particularly at lower volume fractions ($\eta < 0.07$). The last term in Eq. (57) clearly is essential to reduce the rapidly increasing counterion ideal-gas pressure. The discrepancies at higher volume fractions ($\eta > 0.07$) might be attributed, at least partially, to an underestimate of P_m by the liquid-state theory. They may also reflect nonlinear response of the counterions and associated effective many-body interactions between pseudo-macroions. Future work will address influences of effective triplet interactions on the osmotic pressure [42]. It should be mentioned that the Poisson-Boltzmann cell model [12,39] (upper curve in Fig. 1) matches the experimental data well, especially at higher η . However, while cell models, which consider the distribution of microions within a Wigner-Seitz cell centered on a single macroion, are limited to periodic crystals, the more general one-component model applies to any thermodynamic phase.

A more stringent test of the theory is presented by the bulk modulus – the curvature, with respect to density, of the free energy density. In recent experiments, Weiss *et al.* [43] determined the bulk modulus of colloidal fcc crystals suspended in a deionized, aqueous solvent at room temperature ($\lambda_B = 0.714$ nm) by measuring the long-wavelength limit of the static structure factor. For two samples, distinguished by nearest-neighbor distances, $a = (3/4\pi n_m)^{1/3} = 2.5$ μm and 3.25 μm , the measured bulk moduli were argued to be lower than the predictions of DLVO theory, as estimated on the basis of an approximate elastic theory for the macroion contribution, B_m . For the denser crystal, the measured value was $B = 0.016 \pm 0.005$ Pa, less than a third of the estimated “DLVO” value of $B = 0.052 \pm 0.005$

Pa. This analysis ignores, however, the counterion contribution associated with the volume energy. Figures 2 and 3 present predictions, computed from Eq. (58), for the counterion contribution, B_0 . These results demonstrate that for sufficiently high effective macroion charge and volume fraction the counterion contribution may become *negative*. It is essential to include this contribution in the total bulk modulus before comparing the DLVO theory with experiment. In Fig. 2, the cross-over point at $Z^* \simeq 7100$ may be compared with the effective charges, $Z^* \simeq 6100$ for $a = 2.5 \mu\text{m}$ and $Z^* \simeq 5200$ for $a = 3.25 \mu\text{m}$, estimated by Weiss *et al.* for isolated pairs of spheres in the infinite dilution limit. However, lacking reliable knowledge of Z^* in the crystal phase, we forgo here a more quantitative analysis. The qualitative message is nevertheless clear: at sufficient concentration, the counterions may act to *lower* the bulk modulus, softening or even destabilizing ($B < 0$) the crystal.

IV. CONCLUSIONS

In summary, by reducing a model colloidal suspension of charged hard-sphere macroions and point microions to an equivalent one-component system, and approximating the microion response to the macroion charge using linear response (second-order perturbation) theory, we have derived an effective electrostatic pair interaction [Eq. (51)] and an associated microion volume energy [Eq. (55)]. The volume energy, which depends on the average macroion density, accounts for both the microion entropy and the macroion-microion interaction energy. The effective interaction, which governs the dynamics of the macroions, is of precisely the conventional DLVO form for finite-sized macroions, but incorporates excluded volume corrections through the dependence of the screening constant on the *effective* density of microions in the free volume between macroion cores.

The total free energy of the system is the sum of the volume energy and the free energy of the equivalent one-component system of pseudo-macroions. From the free energy, we have derived simple analytic expressions for the osmotic pressure and bulk modulus. Comparison of theoretical predictions with experimental data for deionized suspensions of highly charged macroions shows that the microions can significantly contribute to the thermodynamic properties, beyond their role in screening the bare Coulomb interaction between macroions. In particular, the volume energy largely accounts for the observed magnitude of the osmotic pressure and qualitatively explains measurements of bulk modulus lower than predicted by the conventional one-component DLVO theory. Several recent studies have predicted similar influences of volume energies on the phase behavior of charged colloids [14–17,29].

The theory presented here can be straightforwardly generalized to include *nonlinear* response of microions [42] and thereby used to assess the relative importance of effective *many-body* interactions [13,23,45] and associated corrections to the effective pair potential and the volume energy. Related applications are to colloid-surface interactions and to interactions between colloids in the vicinity of a surface, which experiment [7] and theory [18] suggest may become attractive. Work along these lines is in progress.

ACKNOWLEDGMENTS

I am grateful to Anne M. Denton, Hartmut Löwen, Hartmut Graf, and Christos N. Likos for helpful discussions, and to Luc Belloni for kindly supplying the HNC and PBC data used in Figure 1.

* Permanent address: Dept. of Physics, North Dakota State University, Fargo, ND 58105

-
- [1] R.J. Hunter, *Foundations of Colloid Science* (Oxford University Press, Oxford, 1986).
 - [2] P.N. Pusey, in *Liquids, Freezing and Glass Transition*, session 51, ed. J.-P. Hansen, D. Levesque, and J. Zinn-Justin (North-Holland, Amsterdam, 1991).
 - [3] G. Pan, R. Kesavamoorthy, and S.A. Asher, *Phys. Rev. Lett.* **78**, 3860 (1997).
 - [4] J.H. Holtz and S.A. Asher, *Nature* **389**, 829 (1997).
 - [5] J.E.G.J. Wijnhoven and W.L. Vos, *Science* **281**, 802 (1998).
 - [6] B.V. Derjaguin and L. Landau, *Acta Physicochimica* (USSR) **14**, 633 (1941); E.J.W. Verwey and J.T.G. Overbeek, *Theory of the Stability of Lyophobic Colloids* (Elsevier, Amsterdam, 1948).
 - [7] A.E. Larsen and D.G. Grier, *Nature* **385**, 230 (1997); A.E. Larsen and D.G. Grier, *Phys. Rev. Lett.* **76**, 3862 (1996); J.C. Crocker and D.G. Grier, *Phys. Rev. Lett.* **77**, 1897 (1996).

- [8] K. Ito, H. Yoshida, and N. Ise, *Science* **263**, 66 (1994); B.V.R. Tata, M. Rajalakshmi, and A.K. Arora, *Phys. Rev. Lett.* **69**, 3778 (1992).
- [9] J.S. Rowlinson, *Mol. Phys.* **52**, 567 (1984).
- [10] S. Alexander, P.M. Chaikin, P. Grant, G.J. Morales, and P. Pincus, *J. Chem. Phys.* **80**, 5776 (1984).
- [11] R.J.F. Leote de Carvalho, E. Trizac, and J.-P. Hansen *Europhys. Lett.* **43** 369 (1997).
- [12] M.N. Tamashiro, Y. Levin, M.C. Barbosa *Eur. Phys. J. B* **1**, 337 (1998).
- [13] H. Löwen, P.A. Madden, and J.-P. Hansen, *Phys. Rev. Lett.* **68**, 1081 (1992); *J. Chem. Phys.* **98**, 3275 (1993).
- [14] R. van Roij and J.-P. Hansen, *Phys. Rev. Lett.* **79**, 3082 (1997).
- [15] R. van Roij, M. Dijkstra, and J.-P. Hansen, *Phys. Rev. E* **59**, 2010 (1999).
- [16] R. van Roij and R. Evans, *J. Phys.: Condens. Matter* **11**, 10047 (1999).
- [17] H. Graf and H. Löwen, *Phys. Rev. E* **57**, 5744 (1998).
- [18] D. Goulding and J.-P. Hansen, *Mol. Phys.* **95**, 649 (1998).
- [19] M.J. Stevens, M.L. Falk, and M.O. Robbins, *J. Chem. Phys.* **104**, 5209 (1996).
- [20] E. Allahyarov, I. D'Amico and H. Löwen, *Phys. Rev. Lett.* **81**, 1334 (1998).
- [21] E. Allahyarov, I. D'Amico and H. Löwen, *Phys. Rev. E* **60**, 3199 (1999).
- [22] E. Allahyarov, H. Löwen, and S. Trigger, *Phys. Rev. E* **57**, 5818 (1998).
- [23] H. Löwen and G. Krampposthuber, *Europhys. Lett.* **23**, 673 (1993); R. Tehver, F. Ancilotto, F. Toigo, J. Koplik, and J.R. Banavar, *Phys. Rev. E* **59**, R1335 (1999).
- [24] M.J. Grimson and M. Silbert, *Mol. Phys.* **74**, 397 (1991).
- [25] E. Canessa, M.J. Grimson, and M. Silbert, *Mol. Phys.* **64**, 1195 (1988); in *Strongly Coupled Plasma Physics*, ed. S. Ichimaru (Elsevier/Yamada Science Foundation, 1990), p 675.
- [26] W.A. Harrison, *Pseudopotentials in the Theory of Metals* (Benjamin, New York, 1970); V. Heine, *Solid State Phys.* **24**, 1 (1970).
- [27] J. Hafner, *From Hamiltonians to Phase Diagrams* (Springer, Berlin, 1987).
- [28] N.W. Ashcroft and D. Stroud, *Solid State Phys.* **33**, 1 (1978).
- [29] A.R. Denton and H. Löwen, *Phys. Rev. Lett.* **81**, 469 (1998).
- [30] A.R. Denton, *J. Phys.: Condens. Matter* **11**, 10061 (1999).
- [31] J.-P. Hansen and I.R. McDonald, *Theory of Simple Liquids*, 2nd edition (Academic, London, 1986), Chap. 11.
- [32] M.W. Finnis, *J. Phys. F: Metal Phys.* **4**, 1645 (1974).
- [33] R. Abe, *Prog. Theor. Phys.* **22**, 213 (1959).
- [34] L.D. Landau and E.M. Lifshitz, *Statistical Physics*, Vol. 5 (Pergamon, Oxford, 1980).
- [35] See Ref. [31], Chap. 5.
- [36] W.B. Russel, in *Theory of Dispersed Multiphase Flow*, ed. R.E. Meyer (Academic, New York, 1981); W.B. Russel and D.W. Benzing, *J. Coll. Int. Sci.* **83**, 163 (1981); A.P. Gast, W.B. Russel, and C.K. Hall, *J. Coll. Int. Sci.* **109**, 161 (1986).
- [37] As a check, the calculations were repeated, replacing the bare Coulomb interaction, $e^2/\epsilon r$, by a screened Coulomb interaction $(e^2/\epsilon r) \exp(-\lambda r)$, and taking the $\lambda \rightarrow 0$ limit only at the end. The results are exactly the same, since the uniform compensating background automatically ensures charge neutrality of the microion plasma [14].
- [38] S.M. Ilett, A. Orrock, W.C.K. Poon, and P.N. Pusey, *Phys. Rev. E* **51**, 1344 (1995).
- [39] V. Reus, L. Belloni, T. Zemb, N. Lutterbach, and H. Versmold, *J. Phys. II France* **7**, 603 (1997).
- [40] L. Belloni, private communication.
- [41] M.O. Robbins, K. Kremer, and G.G. Grest, *J. Chem. Phys.* **88**, 3286 (1988).
- [42] A.R. Denton, unpublished.
- [43] J. Weiss, A.E. Larsen and D.G. Grier, *J. Chem. Phys.* **109**, 8659 (1998).
- [44] C.E. Woodward, B. Jönsson, and T. Åkesson, *J. Chem. Phys.* **89**, 5145 (1988); P. Attard, R. Kjellander, and D.J. Mitchell, *J. Chem. Phys.* **89**, 1664 (1988).
- [45] H. Löwen and E. Allahyarov, *J. Phys.: Condens. Matter* **10**, 4147 (1998).

Figure 1

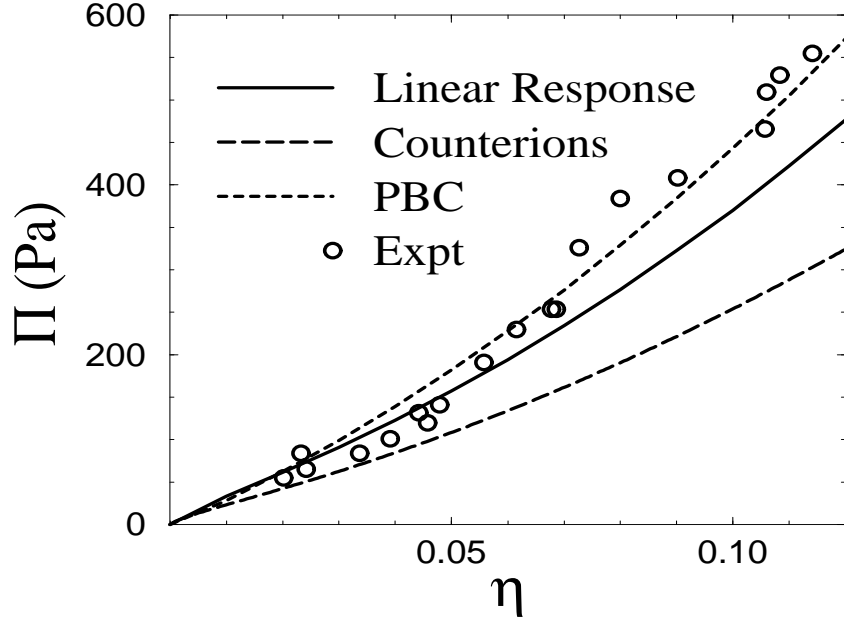


FIG. 1. Osmotic pressure Π vs. macroion volume fraction η for an fcc crystal of spherical macroions (diameter $\sigma = 102$ nm) suspended in a salt-free, aqueous solvent at room temperature ($\lambda_B = 0.714$ nm). Symbols: experimental data of Reus *et al.* [39]; solid curve: prediction of linear response theory [Eq. (57)] with effective macroion charge $Z^* = 700$ and HNC-virial pressure for macroions (see text); long-dashed curve: counterion contribution Π_0 ; short-dashed curve: Poisson-Boltzmann cell model prediction [12,39]. Over this range of volume fractions, the screening constant increases from zero to $\kappa\sigma \simeq 4$.

Figure 2

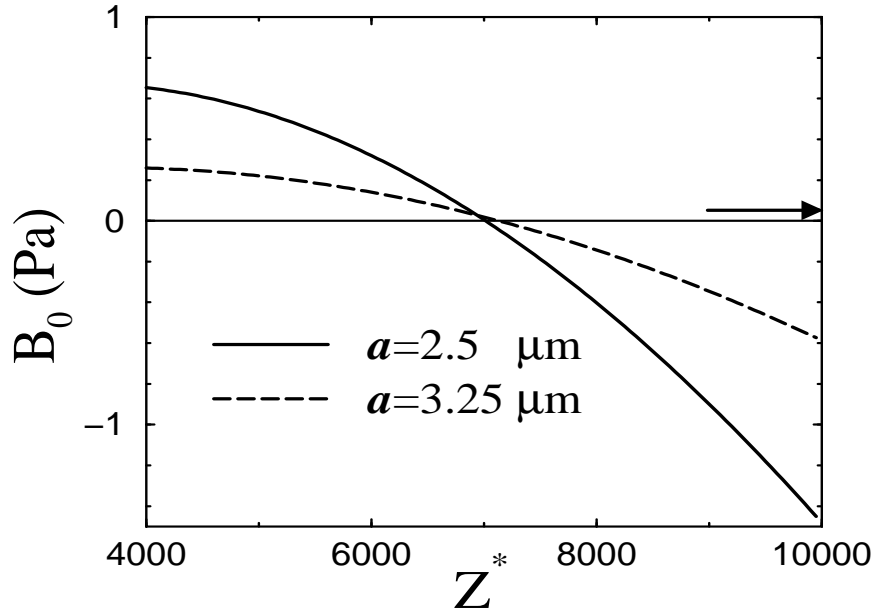


FIG. 2. Counterion contribution to bulk modulus B_0 vs. effective macroion charge Z^* for fcc crystals of spherical macroions (diameter $\sigma = 654$ nm) suspended in a salt-free, aqueous solvent at room temperature. Parameters are chosen for comparison with ref. [43]. Solid curve: nearest-neighbor distance $a = 2.5$ μm (macroion volume fraction $\eta = 0.0133$); dashed curve: $a = 3.25$ μm ($\eta = 0.00475$). For $Z^* > 7100$ the counterion contribution is negative. The arrow indicates the estimated macroion contribution to the bulk modulus of the denser crystal [43] (see text). The maximum screening constant is $\kappa\sigma = 1.9$.

Figure 3

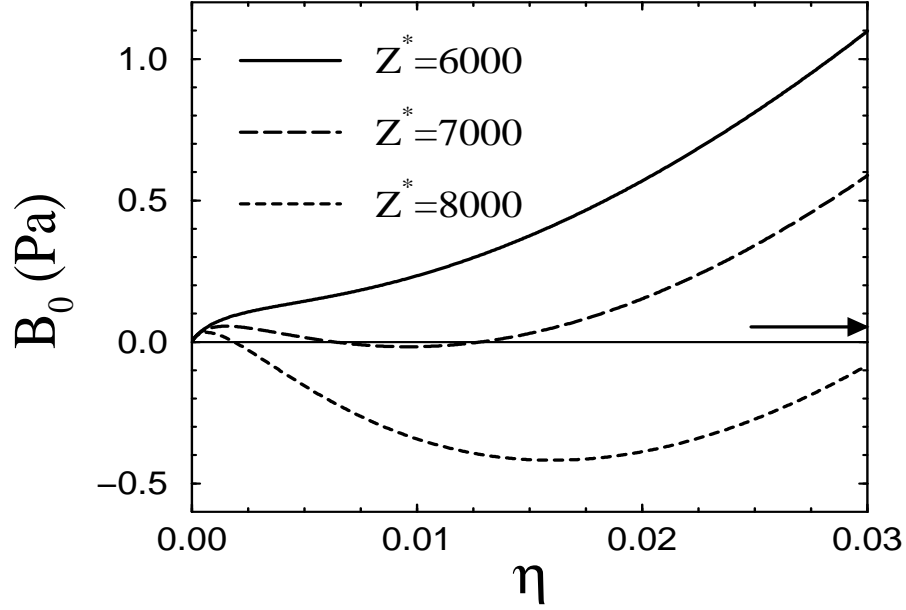


FIG. 3. Counterion contribution to bulk modulus B_0 vs. macroion volume fraction η for same system as in Fig. 2, but for three different effective macroion charges. Solid curve: $Z^* = 6000$; long-dashed curve: $Z^* = 7000$; short-dashed curve: $Z^* = 8000$. For sufficiently high Z^* , the counterion contribution may be negative over a significant range of volume fractions. The arrow indicates the estimated macroion contribution to the bulk modulus of the denser crystal [43]. The maximum screening constant is $\kappa\sigma = 2.5$.